

SARS-CoV2 mutant-specific T cells and neutralizing antibodies after vaccination and up to 1 year after infection

Jennifer R. Richardson, Ralph Götz, Vanessa Mayr, Martin J. Lohse, Hans-Peter Holthoff*, Martin Ungerer*

*shared senior authorship

ISAR Bioscience, Semmelweisstrasse 5, D 82152 Planegg, Germany

Short title: SARS-CoV2-specific T cells

Key Words: SARS-CoV2

Correspondence to: Prof. Martin Ungerer, MD, or to Hans-Peter Holthoff, PhD, ISAR Bioscience, Semmelweisstrasse 5, D 82152 Planegg, Germany;
martin.ungerer@isarbioscience.de; hans-peter.holthoff@isarbioscience.de

Abstract

Objective: We investigated blood samples from fully SARS-CoV2-vaccinated subjects and from patients up to one year after infection with SARS-CoV2, and compared short and long term T cell and antibody responses, with a special focus on the recently emerged delta variant (B.1.617.2).

Methods and Results: In 23 vaccinated subjects, we documented high anti-SARS-CoV2 spike protein receptor binding domain (RBD) antibody titers. Average virus neutralization by antibodies, assessed as inhibition of ACE2 binding to RBD, was 2.2-fold reduced for delta mutant vs. wt RBD. Specific CD4+ T cell responses as measured using stimulation with peptides representing wt or alpha, beta, gamma and delta variant SARS-CoV2 entire spike proteins by flow cytometric intracellular cytokine staining, did not differ significantly between vaccinees.

One year post infection in one of the earliest SARS-CoV2 populations in the Western world, mean specific antibody titers were lower than in vaccinees; ACE2 binding to delta mutant vs. wt RBD was 1.65-fold reduced. T cell responses, especially interferon gamma expression, to mutant SARS-CoV2 spike were significantly reduced compared to those in vaccinees.

Conclusion: Strong T cell responses occurred for wildtype and mutant SARS-CoV2 variants, including delta (B.1.617.2), in fully vaccinated individuals, whereas they were partly reduced 1 year after natural infection. Antibody neutralisation of delta mutant was reduced compared to wt, as assessed in a novel inhibition assay with a finger stick drop of blood. Hence, immune responses after vaccination are stronger compared to those after naturally occurring infection, pointing out the need of the vaccine to overcome the pandemic.

Introduction

Since December 2019, the SARS-CoV-2 pandemic has caused global health problems, leading to more than 4 million deaths (Johns Hopkins University database) and therefore demanding rapid development of vaccines for protection against the virus. Vaccine development has included mRNA, viral vectors, recombinant proteins and inactivated virus (1), leading to discussions about the efficiency of the various approaches in terms of humoral and cellular immune responses against the virus. Several vaccines have been investigated in large clinical trials and have demonstrated safety and efficacy (2-4): among them, BNT162b2 (Pfizer-BioNTech; mRNA), mRNA-1273 (Moderna; mRNA), and ChAdOx1 nCoV-19 (AZD1222) (Oxford-AstraZeneca; chimpanzee adenoviral vectored) have been approved globally and have been most frequently used in Europe. All of these vaccines have been designed to raise antibodies and T lymphocyte responses to the spike (S) protein, and all include S sequences derived from the first reported sequence from Wuhan in January 2020 (5).

Similar to other RNA viruses, SARS-CoV-2 is subject to progressive mutational changes. The pandemic spread leads to a huge extent of viral replication, increasing the odds that adaptive mutations will occur, which could lead to selective± advantages, e.g. enhanced binding to human cells or immune escape from neutralizing antibodies (6). The S protein is a type-1 transmembrane glycoprotein, which may assemble into trimers (7). It is composed of two parts: the S1 domain bears the receptor-binding domain (RBD) and mediates cell binding via the angiotensin-converting enzyme-2 (ACE2), while the S2 domain completes membrane fusion, allowing the viral RNA to access the host cell cytoplasm to initiate viral replication.

The ACE2-RBD interaction is mediated by a small 25 amino acid patch, which becomes accessible when the RBD moves into an upper direction (8; 9). Mutations in this region are most concerning:

The alpha (B.1.1.7), beta (B.1.351), gamma (P.1) and delta (B.1.617.2) variants have been classified as variants of concern and have by far superseded the wt. These all have the

potential to modulate ACE2-RBD binding affinity, potentially leading to an increased transmissibility. In addition, the variants' mutated amino acid residues can also modulate neutralization of SARS-CoV2 by naturally or vaccine induced antibody responses.

In this study, we therefore compared the immune responses of individuals less than 2 months or 1 year after a naturally occurring infection with SARS-CoV2 with those of subjects who had been completely vaccinated (at least two weeks after the last dose) with either mRNA-based (BNT162b2, Comirnaty (Pfizer-BioNTech), mRNA-1273 (Moderna)) or vector-based vaccines (ChAdOx1 nCoV-19 - Vaxzevria, AZD1222, Oxford-AstraZeneca). We investigated anti-S and anti-N protein antibodies plus inhibition assays of ACE2 binding to wildtype vs. delta mutant RBD proteins (as a correlate of neutralizing potency) and S protein-specific T cell responses to wt and mutant S protein-derived peptide pools. The study was intended to provide further insight into immune responses after naturally occurring infections versus vaccination regarding the most concerning mutant virus variants with a special focus on the delta mutant.

Material and Methods

Research Subjects

Blood was collected from 67 volunteers with informed consent, who had been previously infected with SARS-CoV-2 corona virus or been vaccinated against the virus or been unexposed. SARS-CoV-2 infection was confirmed by PCR testing. Vaccination had been completed with two full doses in all vaccinees, and blood was sampled 5.2 ± 0.9 weeks after the second vaccination. At the time of blood collection, no active infection was present. This project was submitted for ethical review to and approved by the Bavarian Medical Chamber.

SARS-CoV-2-derived Peptides

SARS-CoV-2-derived spike overlapping peptide mixes (15-meric peptides with a 4 amino acid overlap each) from the Wuhan wt strain were purchased from Miltenyi and JPT and from the alpha (B.1.1.7), beta (B.1.351), gamma (P.1) and delta (B.1.617.2) mutant strains were purchased from JPT (PepMix SARS.SMUT01, SMUT02, SMUT03-1, SMUT06-1). The alpha mutant (B.1.1.7) contains the following mutations: H0069-, V0070-, Y0144-, N0501Y, A0570D, D0614G, P0681H, T0716I, S0982A, D1118H, with the RBD including a single N501Y mutation. The beta (B.1.351) variant spike protein contains the mutations D0080A, D0215G, L0242-, A0243-, L0244-, K0417N, E0484K, N0501Y, D614G, A0701V, of which K417N, E484K and N501Y are located within the RBD. In contrast, the gamma mutant (P.1) is characterized by mutations: L018F, T020N, P026S, D138Y, R190S, K417T, E484K, N501Y, D614G, H655Y, T1027I, V1176F, and its RBD displays mutations K417T, E484K and N501Y. The delta variant (B.1.617.2) spike protein is characterized by the following mutations compared to wt: T019R, G142D, E156-, F157-, R158G, L452R, T478K, D614G, P681R and D950N, of which L452R and T478K are part of the RBD. Peptide mixes were dissolved in ddH₂O with or without 1% DMSO (Roth).

Isolation and Freezing of Peripheral Blood Mononuclear Cells and Serum

Blood was collected for peripheral blood mononuclear cell (PBMC) isolation (in S-Monovettes® K3 EDTA (Sarstedt) or equal), as well as for serum isolation (S-Monovettes® Serum (Sarstedt) or equal). The blood was diluted with an equal volume of PBS (Corning) containing 2% fetal bovine serum (FBS; Gibco; heat-inactivated; from Brazil). PBMCs were obtained by density gradient centrifugation using SepMate™-50 tubes (Stemcell Technologies) filled with Lymphoprep™ density gradient medium (Stemcell Technologies) according to the manufacturer's instructions. After the isolation, the PBMCs were stained with Acridine Orange and DAPI (solution 18, Chemometec), counted using the NC-250 cell counter (Chemometec), frozen in FBS with 10% DMSO, and stored in liquid nitrogen for at least one week before further experiments. Blood collected for serum isolation was centrifuged 10 min at 2,000xg. Serum was transferred into Eppendorf tubes and frozen at -20°C until use for further experiments.

T-cell Stimulation and Intracellular Cytokine Staining

Ex vivo T-cell responses were analyzed by intracellular cytokine staining (ICS) after stimulation. To this aim, PBMCs were thawed and rested in T cell medium (TCM; RPMI1640 (+GlutaMAX +HEPES, Gibco) + 8% FBS + 1x Penicillin/Streptomycin (Gibco)) containing 1µg/mL DNase (Sigma) for 4-6 hours at 37°C with 5% CO₂ prior to stimulation. Afterwards, 0.5 - 1.5x10⁶ cells per well (96-well plate) were stimulated with 5 µg/mL of the peptide mixes. DdH₂O with or without DMSO (depending on the solvent of the peptides) and PMA (10µg/mL)/ Ionomycin (1µM) (both from Sigma) were added as negative and positive controls, respectively. The protein transport inhibitor Brefeldin A (10µg/mL, eBioscience) was added simultaneously and cells were incubated for 14-16h at 37°C, 5% CO₂. The next day, cells were washed in PBS + 0.5% BSA (Sigma) and stained extracellularly for 20 min at 4°C (Table 1). Thereafter, cells were fixed with IC Fixation Buffer (Intracellular Fixation & Permeabilization Buffer Set, eBioscience) for 30 min at room temperature. Cells were

washed and 1x permeabilization buffer (dilute 10x permeabilization buffer from the intracellular fixation & permeabilization buffer set, eBioscience with 9x ddH₂O) was added and incubated for 5 min, before intracellular staining for 30 min at room temperature (Table 1). Subsequently, cells were washed twice, resuspended in PBS + 0.5% BSA and analyzed with the MACSQuant10 flow cytometer (Miltenyi).

The data analysis was performed with FCS Express 7 (V. 7.06, De Novo Software). All results were audited, and responses were defined as positive if the percentage of marker-positive cells after peptide stimulation was \geq two-fold compared to the negative control and >20 marker-positive cells were recorded. The frequency of the negative controls was subtracted from the frequency of marker-positive cells.

Enzyme-linked Immunosorbent Assay

Generation of CHO RBD-His and CHO-NP-Strep Cell Lines

S protein RBD-His consists of the amino acids corresponding to the receptor binding (RBD) domain, which was derived from the S protein nucleotide sequence (positions 22517- 23183, amino acids 319 to 541, RVQP....CVNF) of the SARS-CoV2 Wuhan Hu-1 genome (Genbank accession number MN908947) followed by six histidines. Nucleocapsid protein N-strep consists of the amino acids corresponding to the N protein nucleotide sequence (positions 28290 to 29549) of the SARS-CoV2 Wuhan Hu-1 genome (Genbank accession number MN908947) followed by a streptavidin tag (NP-Strep). Accordingly, alpha (B.1.1.7) RBD contains a single N501Y mutation, whereas the beta (B.1.351) variant RBD displays K417N, E484K and N501Y and gamma (P.1) RBD mutations K417T, E484K and N501Y. In contrast, the delta variant (B.1.617.2) spike RBD contains L452R, T478K.

The complementary DNA sequences adapted for hamster codon usage were produced synthetically by GeneArt (Life Technologies) by adding the signal sequence METPAQLLFLLLLWLPDTTG at the beginning and cloned into the plasmid vector

pcDNA5/FRT via BamHI and XhoI. The resulting vectors were called pcDNA5/CoV-RBD-His and pcDNA5/CoV-NP-Strep, respectively, and allow for expression and secretion of RBD-His or NP-Strep into the culture medium of mammalian cells under the control of the human cytomegalovirus (CMV) immediate-early enhancer/promoter. The selection for stable clones was done using Hygromycin B after co-transfection with the plasmid pOG44. The vectors were transfected into Flip-In™-Chinese hamster ovary (CHO) cells (Life Technologies) using the Lipofectamine 2000 Reagent (Invitrogen, #11668-019), together with the plasmid pOG44, providing site-directed recombination. After selection of a stably expressing clone for each line in Ham's F12 medium supplemented with 10% FBS and 600 µg/ml Hygromycin B, the clones were adapted to ProCHO5 medium (Lonza, #BE12-766Q) supplemented with 4 mM L-glutamine (Biochrom, #K0283).

Expression and purification of RBD-His and NP-Strep

The various CHO-spike-RBD-His cells and CHO-spike-NP-Strep cells were grown in suspension in ProCHO5, 4 mM L-glutamine and 600 µg/ml Hygromycin B in flasks to submaximal density at 37°C. The supernatants were collected after centrifugation at 400xg for 5 min and subsequent filtration with a 0.22 µm sterile filter (TPP, #99722). The resulting RBD-His or NP-Strep protein-containing medium was immediately frozen and stored at -20°C until protein purification. The cells were continuously grown at 37°C, with splitting and supernatant collection every 3 – 4 days.

For protein purification, thawed CHO-RBD-His supernatants (1 L) were loaded onto an equilibrated 1 ml HisTrap™ excel column (GE Healthcare 17-3712-05). After washing the column with wash buffer (20 mM sodium phosphate, 0.3 M NaCl, pH 8.0), RBD-His was eluted with 4 x 1 ml 0.25 M imidazole, 20 mM sodium phosphate, 0.3 M NaCl, pH 8.0. Protein concentration and, hence, content was determined by OD 280 measurement and the relevant fractions were dialyzed (Slide-A-Lyzer Dialysis Cassette, 10000 MWCO, Thermo Scientific # 66380) against phosphate-buffered saline (PBS from Roth: 137 mM NaCl, 2.7

mM KCl, 10 mM Na₂HPO₄, 2 mM KH₂PO₄, pH 7.4, 0.2 µm filtered and steam sterilized) at 4°C for 16 h.

0.5 L CHO-NP-Strep supernatants were diluted 1:2 in 50 mM sodium phosphate, 0.3 M NaCl, pH 8.0, and loaded on an equilibrated 1 ml StrepTrap™ HP column (GE Healthcare 28-9075-46). After washing the column with 50 mM sodium phosphate, 0.3 M NaCl, pH 8.0, NP-Strep was eluted with 4 x 1 ml 20 mM sodium phosphate, 0.3 M NaCl, 2.5 mM desthiobiotin (Sigma, # D 1411) pH 8.0. Protein content was determined by OD 280 measurement and the relevant fractions were dialyzed (Slide-A-Lyzer Dialysis Cassette, 10000 MWCO, Thermo Scientific # 66380) against PBS at 4°C for 16 h.

For biotinylation of RBD, delta mutantRBD or ACE2, the EZ-Link Micro Sulfo-NHS-LC biotinylation kit (Thermo Scientific # 21935 or #A39257) was used with 20-fold molar excess according the standard procedure instruction, followed by removal of excess biotin by dialysis against 1 l PBS for 16 h at 4°C, using Slide-A-Lyzer™ Dialysis Cassettes, 7K MWCO, 0.5 mL (ThermoFisher # 66373).

Qualitative Detection of anti-SARS-CoV2 Antibodies in Human Serum

Anti-SARS-CoV2 antibodies in human serum or in a drop of full blood were detected by a two-step incubation antigen sandwich ELISA using the RBD of the S1 protein of the SARS-CoV2 virus. All procedures were performed at room temperature (RT) and incubations were done on a microtiter plate shaker. ELISA plates were coated with 60 µl/ well RBD-His protein (final concentration 0,45 µg/ml) in coating solution (Candor, #121125) for 1 h. The coated plates were washed three times with PBST (PBS, 0.1 % Tween-20), blocked with 100 µl/well of blocking solution (PBST, 3 % milk powder) for 1 h, and washed again. 30µl serum samples were diluted 1:2, 1:20, 1:200 and 1:2000 with PBS and transferred to the blocked ELISA plates and incubated for 1h. After washing three times with PBST, the ELISA plates were incubated for 1h with 60 µl/well of biotinylated RBD-His (Bio-RBD-His, final concentration 0.02 µg/ml, diluted in PBST). The plates were washed three times with PBST

and incubated with Strep-POD (Jackson ImmunoResearch, #016-030-084) diluted in PBST 1:50000 for 1h. After washing five times, bound POD was detected by incubation with 100 μ l/ well of TMB substrate (Thermo Scientific, #34029) until a maximal optical density (OD) of about 1 to 2 was reached. Finally, the colorimetric reaction was stopped with 100 μ l/ well stopping solution (1M H₂SO₄) and the OD determined at a wavelength of 450 nm with a reference wavelength of 595 nm in a plate reader.

Neutralisation of wt RBD-Biotin binding vs. delta mutant RBD-Biotin binding to immobilized ACE2-His by serum antibodies

All procedures were performed at room temperature (RT) and incubations were done on a microtiter plate shaker. ELISA plates were coated with 60 μ l/ well ACE2-His protein with 1 μ g/ml in PBS for 1 h. The coated plates were washed three times with PBST (PBS, 0.1 % Tween-20), blocked with 100 μ l/well of blocking solution (PBST, 3 % milk powder) for 1 h, and washed again. 60 μ l of RBDwt-Bio (0,3 μ g/ml) or RBDdelta-Bio (0,3 μ g/ml) were co-incubated with various serum sample dilutions (1:2, 1:4, 1:8, 1:16, 1:48, 1:160, 1:1480, 1:1600 in PBST) and transferred to the blocked ELISA plates and incubated for 1h. The plates were washed three times with PBST and incubated with Strep-POD (Jackson ImmunoResearch, #016-030-084) diluted in PBST 1:20000 for 1h. After washing four times, bound POD was detected by incubation with 100 μ l/ well of TMB substrate (Thermo Scientific, #34029) until a maximal optical density (OD) of about 1 to 2 was reached. Finally, the colorimetric reaction was stopped with 100 μ l/ well stopping solution (1M H₂SO₄) and the OD determined at a wavelength of 450 nm with a reference wavelength of 595 nm with in a plate reader.

Then, IC₅₀ values minus blank values were calculated for each sample using results from all dilutions with SigmaPlot v14.5. These IC₅₀ values represent neutralizing serum dilutions. Ratios between IC₅₀s calculated for inhibition of wt vs. delta mutant RBD binding to immobilized ACE2 were used for further analysis.

Neutralisation of ACE2-Biotin binding to immobilized wt RBD vs. delta mutant RBD by serum antibodies

All procedures were performed at room temperature (RT) and incubations were done on a microtiter plate shaker. ELISA plates were coated with 60 µl/ well RBDwt protein or RBDdelta with 2 µg/ml in coating buffer (50mM carbonate buffer, Na₂CO₃/NaHCO₃, pH9.6) for 1 h. The coated plates were washed three times with PBST (PBS, 0.1 % Tween-20), blocked with 100 µl/well of blocking solution (PBST, 3 % milk powder) for 1 h, and washed again. 60µl of ACE2-Bio with 0,3µg/ml was co-incubated with various serum sample dilutions (1:2, 1:4, 1:8, 1:16, 1:48, 1:160, 1:1480, 1:1600 in PBST) and transferred to the blocked ELISA plates and incubated for 1h. The plates were washed three times with PBST and incubated with Strep-POD (Jackson Immunoresearch, #016-030-084) diluted in PBST 1:20000 for 1h. After washing four times, bound POD was detected by incubation with 100 µl/ well of TMB substrate (Thermo Scientific, #34029) until a maximal optical density (OD) of about 1 to 2 was reached. Finally, the colorimetric reaction was stopped with 100 µl/ well stopping solution (1M H₂SO₄) and the OD determined at a wavelength of 450 nm with a reference wavelength of 595 nm with in a plate reader.

Then, IC₅₀ values minus blank values were calculated for each sample using results from all dilutions with SigmaPlot v14.5. These IC₅₀ values represent neutralizing serum dilutions. Ratios between IC₅₀s calculated for inhibition of ACE2 binding to immobilized wt vs. delta mutant RBD were used for further analysis.

Statistical Analysis

Statistical analysis was performed using SPSS software version 26. Statistical differences were determined using one-way ANOVA with Tukey's post-hoc test in case data were

normally distributed (as assessed by Shapiro-Wilk normality test). Otherwise, data were analyzed using the Kruskal-Wallis nonparametric test.

Results

SARS-CoV2 mutant spike RBD and nucleocapsid wild type and mutant proteins were expressed in mammalian cells and purified to > 99% purity to be used in the assays. Figures 1A + B show representative examples for the purity after the affinity column and after subsequent dialysis, respectively.

All vaccinees showed clear antibody responses against wildtype SARS-CoV2 RBD. This finding occurred regardless of the type of vaccine used – as shown in Figure 2A. We did not detect any anti-nucleocapsid protein antibodies in any vaccinated subjects, except in one subject which had suffered from naturally occurring infection before vaccination.

In comparison, we assessed short-term and long-term immune responses in patients' blood samples up to one year after infection with SARS-CoV2 (Figure 2A). We found specific anti-SARS-CoV2 RBD spike protein and anti-nucleocapsid antibody titers in 90% investigated individuals, as assessed by comparing these titers with non-specific protein binding on the plates. Titers in vaccinees were significantly higher than in subjects after natural infection, regardless of the time interval since infection.

Also, inhibition of either wildtype SARS-CoV2 RBD or delta mutant RBD binding to ACE2 was investigated as a correlate for antibody neutralizing potency. We found significantly reduced mean IC₅₀-values for the delta mutant – see Figures 2B-E. Figure 2B shows absolute IC₅₀-values for the inhibition of ACE2 binding to immobilized wt vs. delta mutant RBD, and Figure 2C absolute IC₅₀-values calculated for the inhibition of wt vs. delta mutant RBD binding to immobilized ACE2. The ratios between IC₅₀-values calculated for inhibition of ACE2 binding to immobilized wt vs. delta mutant RBD are shown in Figure 2D. Figure 2E shows ratios between IC₅₀-values calculated for inhibition of wt vs. delta mutant RBD binding to immobilized ACE2. Both, vaccinees and naturally infected subjects showed significantly ($p < 0.001$ by sign testing) reduced mean IC₅₀-values for the delta mutant, with an average 2,2-fold reduction in vaccinees and an 1,65-fold average reduction in the

naturally infected group. Figure 2F shows that results using a drop of finger-stick full blood (about 30 μ l) were well comparable to those using sera obtained by venous puncture.

In summary, results from the inhibition assays were comparable, regardless whether RBD or ACE2 was coated onto plates, and whether RBD or ACE was biotinylated and added in solution – and that the assay can be performed with just a drop of finger-stick blood.

T cell responses were investigated in a first study which showed commonly accepted rates of false negatives and false positives (or inadvertently infected subjects) using a wild type SARS-Cov2 S protein peptide pool derived from the whole amino acid sequence of wildtype protein which was available from the company Miltenyi at the time of the first study (Figure 3). This first study also encompassed vaccinated as well as naturally infected individuals. Similar to results for antibodies, T cell responses to this peptide pool were comparable in all vaccinees regardless of the type of vaccine used. Figure 3 shows the mean activation patterns of tumour necrosis factor (TNF)-alpha (A), interleukin (IL)-2 (B) and of interferon (IFN)-gamma (C) for all subjects. Significant T cell responses were observed both after vaccination and after natural infection.

Follow-up studies then compared peptide pools whose sequences comprised the whole amino acid sequence of wild type and alpha, beta, gamma and delta spike protein mutants, which were obtained from JPT peptides (Figures 4 – 6). Figure 4 shows the mean activation patterns of interferon (IFN)-gamma, Figure 5 of interleukin (IL)-2 and Figure 6 of tumour necrosis factor (TNF)-alpha for all subjects. Specific antibody reactivity and T cell response to SARS-CoV2 mutants alpha, beta, gamma and delta were comparable to wild type in all individuals, with no evidence for reduced responsiveness to any of the mutants (Figures 4 - 6). In comparison, we also tested samples of non infected individuals who were all identified as negative (not shown in the Figure 4 – 6 to enhance legibility). In contrast, significantly reduced T cell responses were observed 1 year after naturally occurring infection compared to vaccines for stimulation: especially, alpha-, beta-, gamma and delta mutant S protein peptide-induced IFN-gamma responses, but also alpha-, beta- and delta mutant-induced IL-2

responses and beta- and delta-induced TNF-alpha responses were significantly lower in subjects which had been infected 1 year before.

We also calculated comparisons of mean T cell responses (TNF alpha and IL-2) with mean anti-RBD and anti-N antibody titers of each group. We observed no relevant correlation between parameters in either vaccinated subjects nor in individuals after naturally occurring infection.

Discussion

All SARS-CoV2 vaccinated individuals showed strong immune reactions in terms of serum antibody binding to wild type and mutant virus proteins and of T cell reactivity against wild type and mutant variant peptide pools, including significant T cell responses against the recently emerged gamma (P.1) and delta (B.1.617.2) variants. Most responses were higher than those of patients up to one year after naturally occurring infection. Especially the results on the delta variant show that a combination of rapid mammalian cell protein expression and adaptive T cell assays allows for quick investigation of immune responses to virus variants within 3 months after their emergence – which may be done even quicker for future variants of concern.

Previous studies investigated antibody responses against SARS-CoV2 after COVID-19, and found decreases of antibody titers over time, that were assumed to correlate with decreasing immunity (10,11). Several recent studies investigated the long-term immune response after naturally occurring SARS-CoV2 infection or vaccination more broadly, including CD4 helper and CD8 effector T cells, memory B cells and others (12-14). Following up on these recent studies, we investigated another cohort in the Munich area, Bavaria, Germany. Specifically, we measured antibody and T cell responses to S protein of recent variants of concern. The values reflect mean immune responses in the groups, whereas individual sera may contain proportions of antibodies to neutralizing epitopes that are sometimes conserved between strains.

Our results show reduced inhibition of delta mutant RBD – ACE2 interaction compared to wild type. To our knowledge, our study systematically compared for the first time inhibition assays which used labelled wt vs. mutant RBD and coated ACE2 on plates with those in which ACE2 was labelled and added in solution to wt vs. mutant RBD-coated plates. The results were comparable for the specific assay conditions which we established – this novel approach enables wide-scale multiplex-compliant assays. Both the direct interaction of anti-SARS-CoV2 serum antibodies of vaccinated or naturally infected subjects with RBD, and the

inhibition exerted by these antibodies on wt versus delta mutant RBD – ACE2 binding were measured by ELISA. The results using a drop of finger-stick full blood (about 30 µl) were well comparable to those using sera obtained by venous puncture, indicating that the assay can be up-scaled to a rapid point-of-care ELISA.

Our findings corroborate other recent studies which investigated delta mutant RBD by assays using live (pseudo)virus (15-19), and resulted in comparable ratios of delta mutant versus wild type binding. However, these assays are time-consuming and require specialized laboratory know-how. Although assessment of neutralization using in vitro binding assays may not reliably predict the potency of immune protection afforded by natural infection or immunization by real SARS-CoV-2, it can be carried out in non-specialized laboratories, and recent results using authentic virus largely substantiate the comparability (20). In over 90% of vaccinees, neutralizing titres (NT50) remained well above the level associated with immune protection in recent vaccine trials (20,21). However, in many individuals post COVID-19 and recipients of a single dose of vaccine – neutralization capacity dropped. Reduced cross neutralization was observed against many virus variants and may impact on vaccine efficacy.

Generally, reduced anti-virus antibody neutralization as observed in vitro does not directly prove vaccine failure (22-24), because other immune mechanisms, especially T cell responses, also contribute significantly to virus inactivation and elimination. For example, infection with influenza virus results in reduced disease upon subsequent infection with other strains, in both human and animal challenge studies, implying the importance of cellular immune mechanisms on protection elicited by vaccination (23).

Therefore, we also investigated T cell responses using peptide pools which were derived from the whole S sequence. This approach allowed for a broader investigation of anti-S protein immune responses. Generally, T cell responses to SARS-CoV2 are known to target a wide range of regions in the spike protein (25, 26). We found that significant immune responses were elicited by all investigated vaccines including mRNA (Moderna and BioNtech), and the vector-based vaccination with Vaxzevria (AstraZeneca). Our results show

strong and comparable specific T cell responses to alpha (B1.1.7), beta (B1.351), gamma (P.1) and delta (B.1.617.2) spike protein variants in vaccinated subjects after two doses.

The correlation between individual specific T cell responses and anti-RBD antibodies was low, probably because B and T cell interaction is not linear, in accordance with previous studies (21).

Our results demonstrate that a combination of fast expression of recombinant proteins in mammalian cell systems and adaptive T cell assays allows for quick investigation of immune responses to virus variants within 3 months after their emergence, and may be possible within 6 weeks for future mutants. Identification of immune reactions against the current virus mutants and future variants of concern will allow to adapt vaccine strategies in order to provide population protection against the emerging lineages of concern of SARS-CoV-2. Our results imply that additional vaccination should be considered after natural infection with SARS-CoV2 in view of global mutant spread. The study summarizes a complementary diagnostic panel to assess immune reactions to vaccines.

Disclosure summary: All authors are employees of the biotech company ISAR Bioscience GmbH

References

1. Krammer F. SARS-CoV-2 vaccines in development. *Nature* 2020; 586: 516–527
2. Polack FP, et al. Safety and Efficacy of the BNT162b2 mRNA Covid-19 Vaccine. *N Engl J Med* 2020; 383: 2603–2615.
3. Baden LR, et al. Efficacy and Safety of the mRNA-1273 SARS-CoV-2 Vaccine. *N Engl J Med* 2020; 384: 403-416
4. Voysey M, et al. Safety and efficacy of the ChAdOx1 nCoV-19 vaccine (AZD1222) against SARS-CoV-2: an interim analysis of four randomised controlled trials in Brazil, South Africa, and the UK. *Lancet*. 2020; 397: 99-111.
5. Long QX, et al. Genomic characterisation and epidemiology of 2019 novel coronavirus: implications for virus origins and receptor binding. *Lancet* 2020; 395: 565–574
6. Volz E, et al. Evaluating the Effects of SARS-CoV-2 Spike Mutation D614G on Transmissibility and Pathogenicity. *Cell* 2021; 184: 64-75.e11
7. Walls AC, et al. Structure, Function, and Antigenicity of the SARS-CoV-2 Spike Glycoprotein. *Cell* 2020; 181: 281-982 292.e6
8. Hoffmann M, et al. SARS CoV-2 Cell Entry Depends on ACE2 and TMPRSS2 and Is Blocked by a Clinically Proven Protease Inhibitor. *Cell* 2020; 181: 271-280e8
9. Shang J, et al. Structural basis of receptor recognition by SARS-CoV-2. *Nature* 2020; 581: 221–224
10. Kreer C, et al. Longitudinal Isolation of Potent Near-Germline SARS-CoV-2-Neutralizing Antibodies from COVID-19 Patients. *Cell* 2020; 182, 843–854.e12. doi:10.1016/j.cell.2020.06.044
11. Rodda LB, et al. Functional SARS-CoV-2-Specific Immune Memory Persists after Mild COVID-19. *Cell* 2021; 184, 169–183.e17. doi:10.1016/j.cell.2020.11.029
12. Ogbe A, et al. T cell assays differentiate clinical and subclinical SARS-CoV-2 infections from cross-reactive antiviral responses. *Nat Commun* 2021; 12: 2055. <https://doi.org/10.1038/s41467-021-21856-3>
13. Wang Z et al. Naturally enhanced neutralizing breadth against SARS-CoV-2 one year after infection. *Nature* 2021; <https://doi.org/10.1038/s41586-021-03696-9>
14. Bilich T, et al. T cell and antibody kinetics delineate SARS-CoV-2 peptides mediating long-term immune responses in COVID-19 convalescent individuals. *Sci Transl Med* 2021;13 (590) eabf7517; doi: 10.1126/scitranslmed.abf7517

15. Choi A, et al. Serum Neutralizing Activity of mRNA-1273 against SARS-CoV-2 Variants. *BioRxiv* preprint posted on June 28, 2021
16. Liu J, et al. BNT162b2-elicited neutralization of B.1.617 and other SARS-CoV-2 variants. *Nature*. 2021;596(7871):273-275. doi: 10.1038/s41586-021-03693-y.
17. Carreño JM, et al. Reduced neutralizing activity of post-SARS-1 CoV-2 vaccination serum against variants B.1.617.2, B.1.351, B.1.1.7+E484K and a sub-variant of C.37. *medRxiv* preprint doi: <https://doi.org/10.1101/2021.07.21.21260961>; posted on July 23, 2021
18. Planas D, et al. Reduced sensitivity of SARS-CoV-2 variant Delta to antibody neutralization. *Nature* 2021; published on July 8, 2021; <https://doi.org/10.1038/s41586-021-03777-9>
19. Kim S, et al. Differential Interactions Between Human ACE2 and Spike RBD of SARSCoV-2 Variants of Concern. *bioRxiv* preprint doi: <https://doi.org/10.1101/2021.07.23.453598>
20. Skelly DT, et al. Vaccine-induced immunity provides more robust heterotypic immunity than natural infection to emerging SARS CoV-2 variants of concern. *Research Square* 2021; <https://doi.org/10.21203/rs.3.rs-226857>
21. Payne RP, et al., Sustained T cell immunity, protection and boosting using extended dosing intervals of BNT162b2 mRNA vaccine. Pre-publication 2021. https://www.pitch-study.org/PITCH_Dosing_Interval_23072021.pdf
22. Gooch KE, et al. Heterosubtypic cross-protection correlates with cross-reactive interferon-gamma secreting lymphocytes in the ferret model of influenza. *Sci. Rep.* 2019; 9, 1–10
23. Sridhar S, et al. Cellular immune correlates of protection against symptomatic pandemic influenza. *Nature Med* 2013; 19:1305-1312. doi:10.1038/nm.3350
24. Wilkinson TM, et al. Preexisting influenza-specific CD4 + T cells correlate with disease protection against influenza challenge in humans. *Nat Med* 2012; 18, 274–280
25. Lumley SF, et al. Antibody Status and Incidence of SARS-CoV-2 Infection in Health Care Workers. *N Engl J Med* 2020; doi:10.1056/nejmoa2034545
26. Grifoni, A et al. Targets of T Cell Responses to SARS-CoV-2 Coronavirus in Humans with COVID-19 Disease and Unexposed Individuals. *Cell* 2020; 181, 1489-1501.e15

Figure Legends

Figure 1

A: Representative Coomassie gel electrophoresis (left panel) and silver stain (right panel) of SARS-CoV2 wild type spike RBD protein (A) and of nucleocapsid protein (B).

Figure 2: Antibodies

The Figure shows results of n=13 independent individuals after vaccination with BioNtech (grey), n=5 Moderna (blue), n=5 AstraZeneca (AZ, red), and n=10 independent individuals one year (orange), and n=7 subjects < 2 months (green) after natural infection with standard errors of the mean (SEM). Significance was tested by one-way ANOVA (A) or by Kruskal-Wallis test for non-parametric values (B-E). **p < 0.05 vs. naturally infected subjects.

A: Anti RBD antibody titres; **B:** Absolute IC50-values calculated for the inhibition of biotinylated ACE2 binding to immobilized wt vs. delta mutant RBD. **C:** Absolute IC50-values calculated for the inhibition of biotinylated wt vs. delta mutant RBD binding to immobilized ACE2. **D:** Ratios between IC50-values calculated for inhibition of ACE2 binding to immobilized wt vs. delta mutant RBD. **E:** Ratios between IC50-values calculated for inhibition of wt vs. delta mutant RBD binding to immobilized ACE2. **F:** Read-out of a representative experiment showing the comparison between inhibition of biotinylated ACE2 binding to immobilized RBD with serum taken by venous sampling vs a drop of full blood.

Figure 3

Specific T cell responses elicited by the Miltenyi S protein peptide pool after vaccination with BioNtech (grey), Moderna (blue) or AstraZeneca (red), or one year (orange) or < 2 months (dark green) after naturally occurring infection with SARS-CoV2. In comparison, samples of healthy control subjects, who tested negative for SARS-CoV2-antibodies, are shown on the right of each panel. The Figure shows relative mean activation patterns of (A) tumour necrosis factor-alpha (TNF), (B) interleukin-2 (IL-2) and (C) interferon-gamma (IFN).

The Figure shows results of n=13 independent individuals after vaccination with BioNtech, n=5 Moderna, n=5 AstraZeneca (AZ), and n=10 independent individuals one year and n=7 subjects < 2 months after natural infection with standard errors of the mean (SEM). For comparison, 27 negative healthy controls were included. Significance levels were tested by Kruskal-Wallis test for non-parametric values.

**p < 0.01 vs. healthy controls

Figure 4

Specific T cell responses elicited by the JPT peptide S protein pools after vaccination with BioNtech (grey), Moderna (blue) or AstraZeneca (red), or one year (orange) or < 2 months (dark green) after naturally occurring infection with SARS-CoV2. The Figure shows relative mean activation patterns of interferon-gamma (IFN) for wildtype, and for alpha (B.1.1.7), beta (B.1.351), gamma (P.1) and delta (B.1.617.2) mutants.

The Figure shows results of n=13 independent individuals after vaccination with BioNtech, n=5 Moderna, n=5 AstraZeneca (AZ), and n=10 independent individuals one year and n=7 subjects < 2 months after natural infection with standard errors of the mean (SEM). Samples of non infected individuals tested negative (not shown in the Figure to enhance legibility). Significance levels were tested with Kruskal-Wallis test for non-parametric samples.

*p < 0.05 vs. healthy controls; **p < 0.01 vs. healthy controls and p < 0.05 vs 1 year after infection

Figure 5

Specific T cell responses elicited by the JPT peptide S protein pools after vaccination with BioNtech (grey), Moderna (blue) or AstraZeneca (red), or one year (orange) or < 2 months (dark green) after naturally occurring infection with SARS-CoV2. The Figure shows relative mean activation patterns of interleukin-2 (IL-2) for wildtype, and for alpha (B.1.1.7), beta (B.1.351), gamma (P.1) and delta (B.1.617.2) mutants.

The Figure shows results of n=13 independent individuals after vaccination with BioNtech, n=5 Moderna, n=5 AstraZeneca (AZ), and n=10 independent individuals one year and n=7 < 2 months after natural infection with standard errors of the mean (SEM). Samples of non infected individuals tested negative (not shown in the Figure to enhance legibility). Significance levels were tested by Kruskal-Wallis test for non-parametric values. **p < 0.01 vs. healthy controls, and p < 0.05 vs. 1 year after infection

Figure 6

Specific T cell responses elicited by the JPT peptide S protein pools after vaccination with BioNtech (grey), Moderna (blue) or AstraZeneca (red), or one year (orange) or < 2 months (dark green) after naturally occurring infection with SARS-CoV2. The Figure shows relative mean activation patterns of tumour necrosis factor alpha (TNF) for wildtype, and for alpha (B.1.1.7), beta (B.1.351), gamma (P.1) and delta (B.1.617.2) mutants.

The Figure shows results of n=13 independent individuals after vaccination with BioNtech, n=5 Moderna, n=5 AstraZeneca (AZ), and n=10 independent individuals one year and n=7 < 2 months after natural infection with standard errors of the mean (SEM). Samples of non

infected individuals tested negative (not shown in the Figure to enhance legibility).

Significance levels were tested by Kruskal-Wallis test for non-parametric values.

* $p < 0.05$ vs. healthy controls, ** $p < 0.01$ vs. healthy controls, and $p < 0.05$ vs. 1 year after infection

Figure 1:

A:

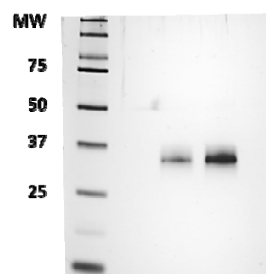
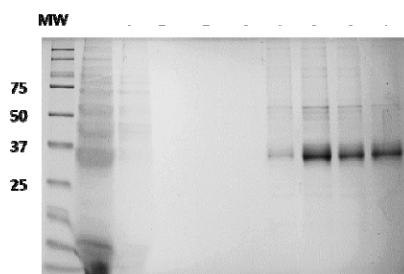


Figure 1B:

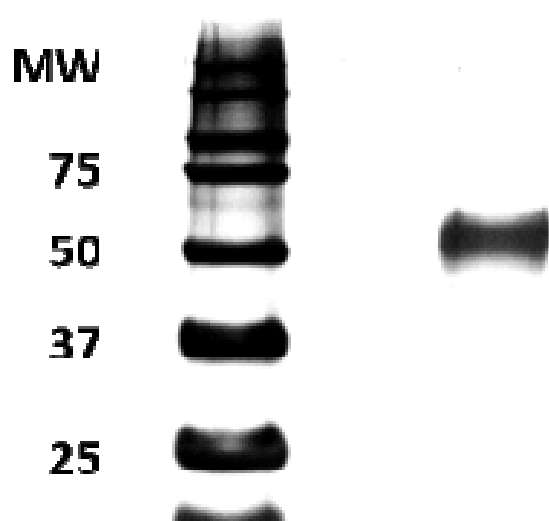
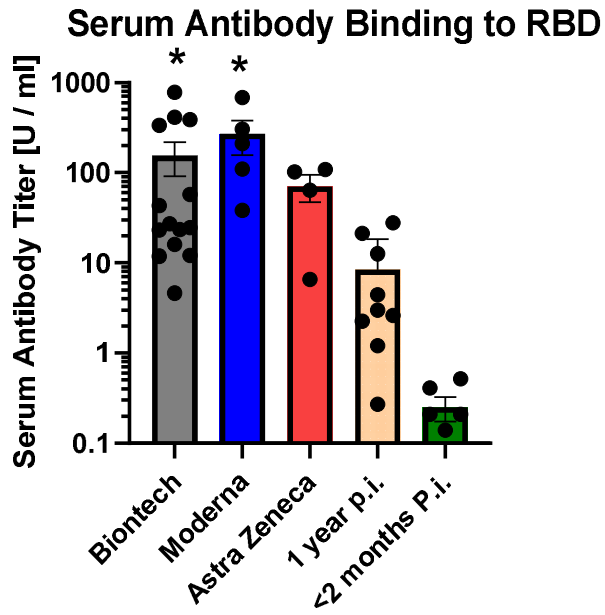
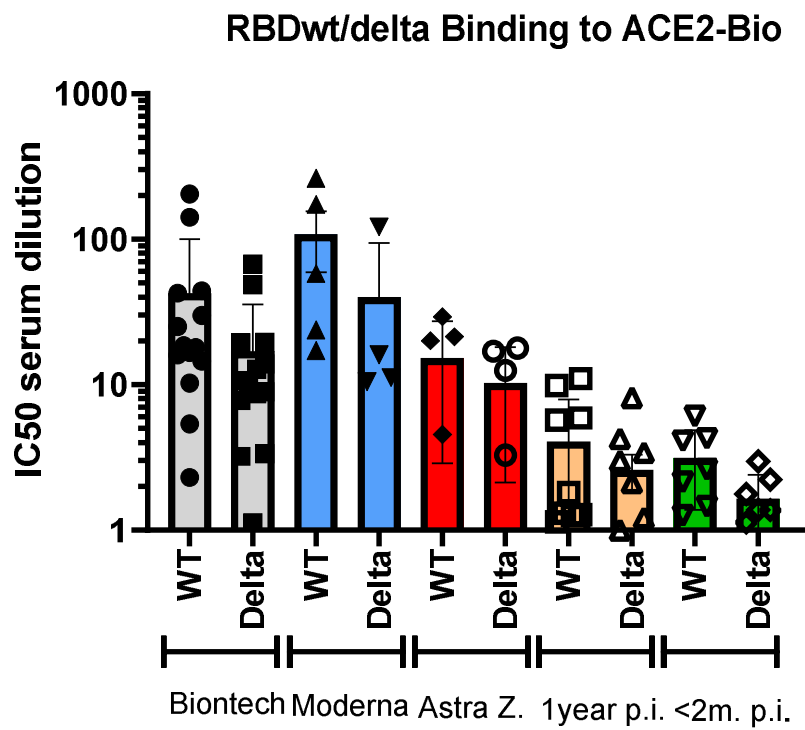


Figure 2:

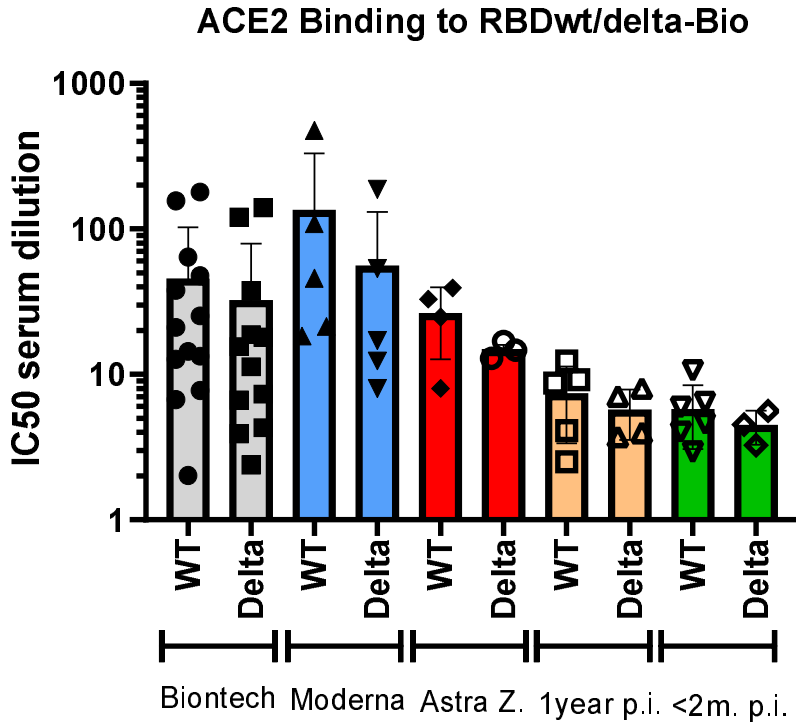
A.



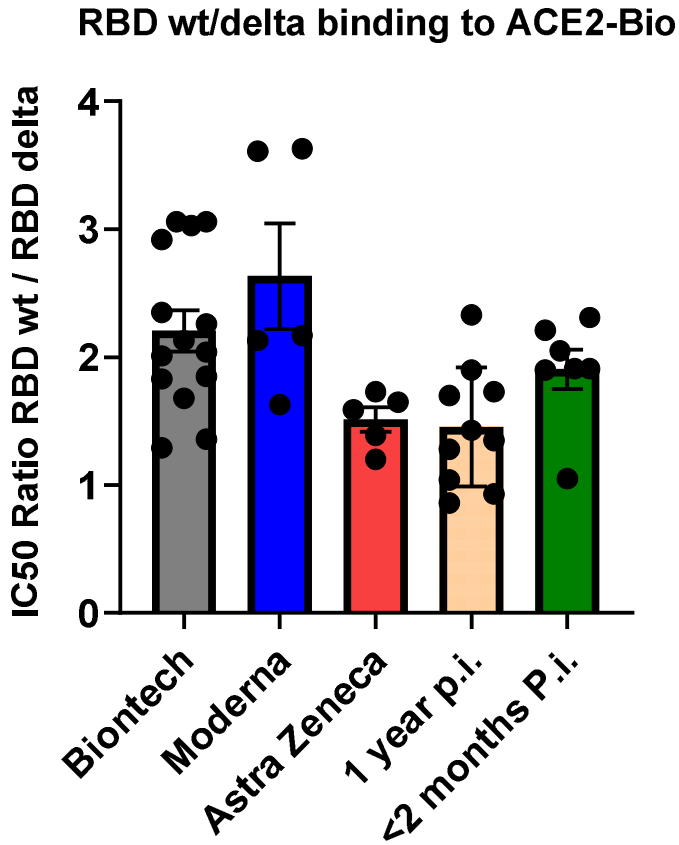
B:



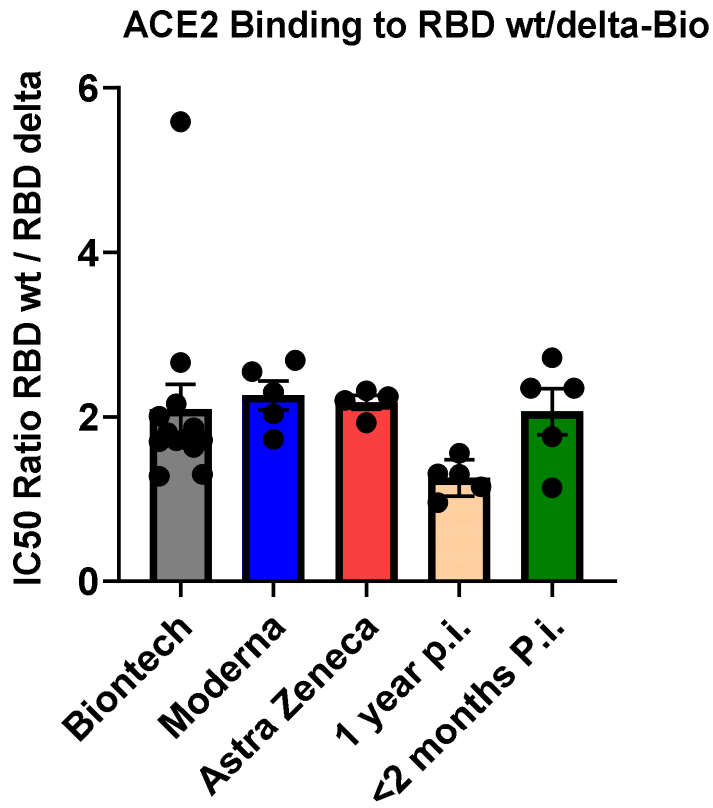
C:



D:



E:



F:

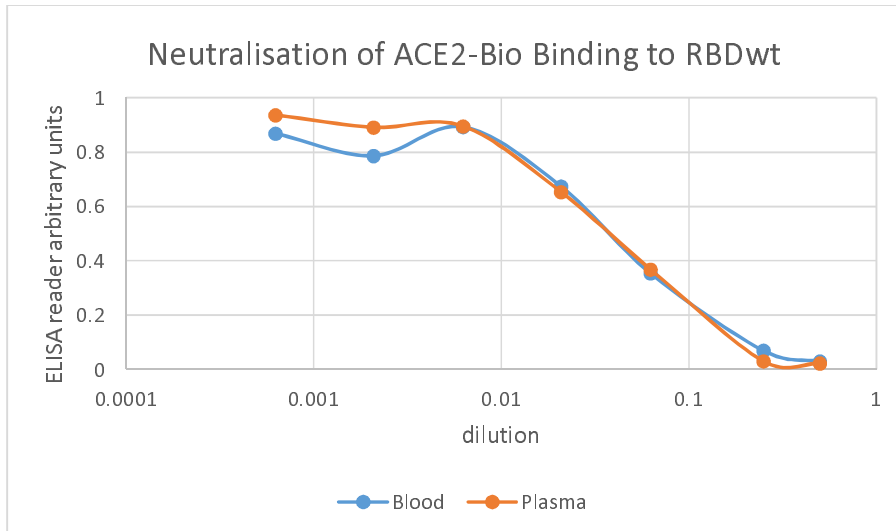
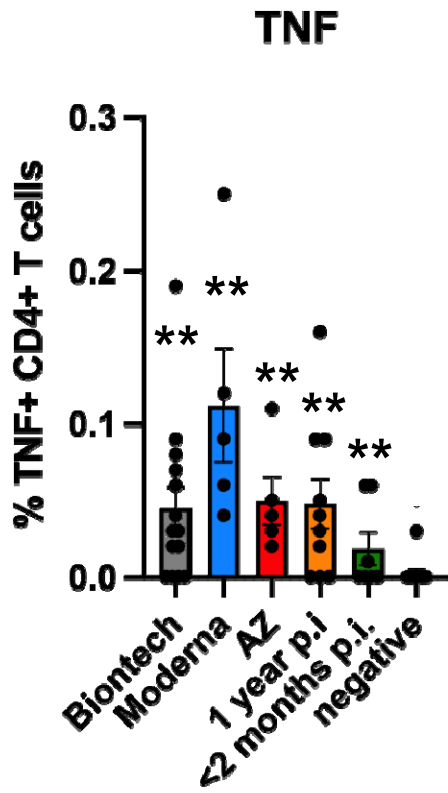


Figure 3: A:



B:

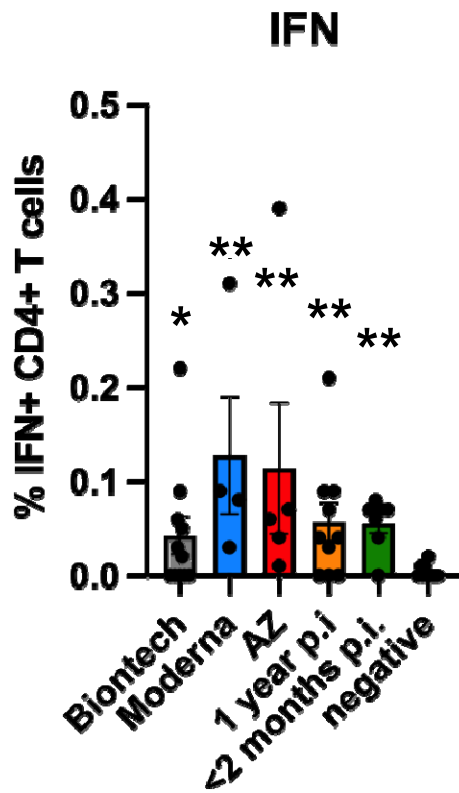
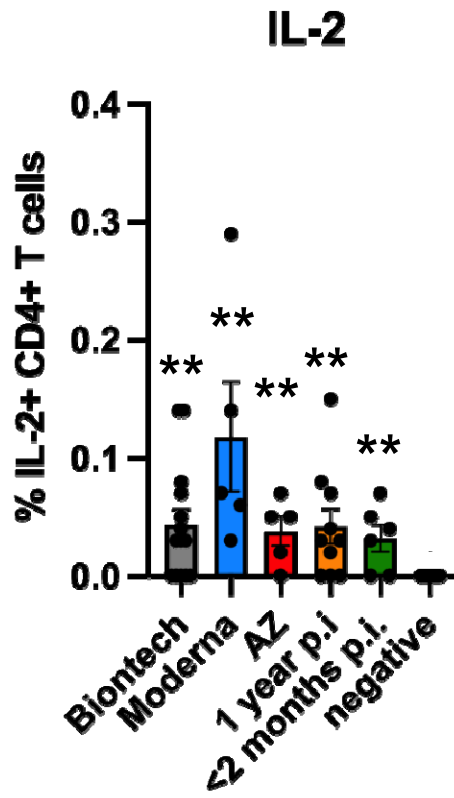


Figure 4:

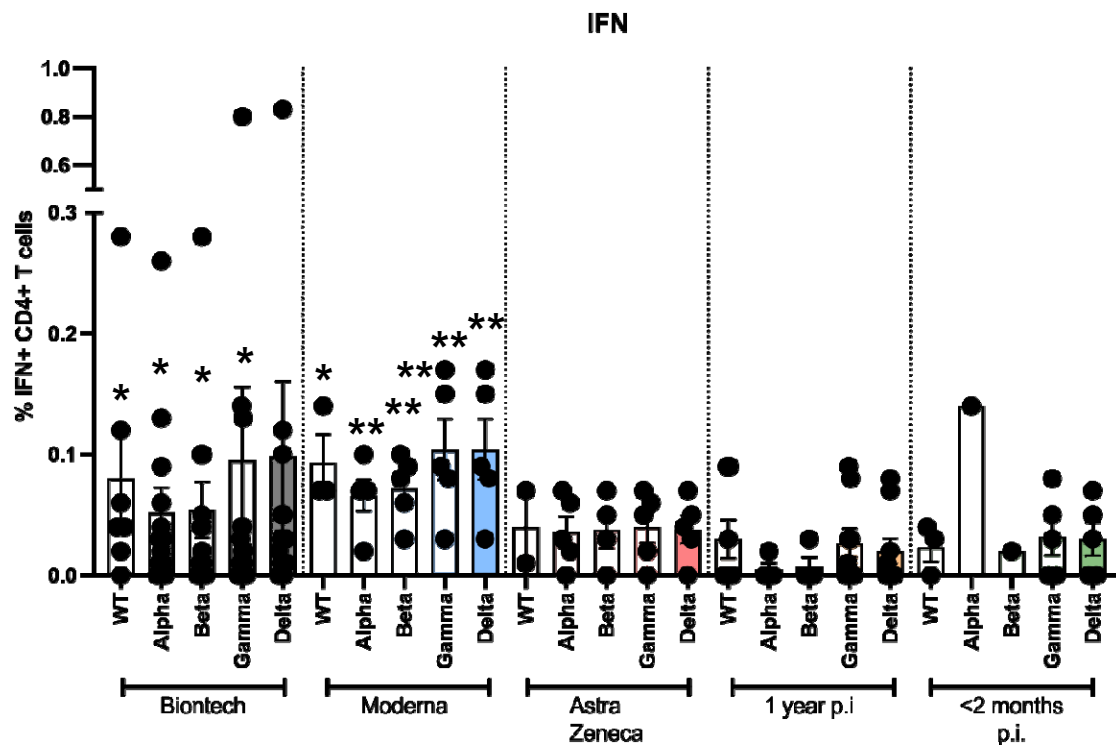


Figure 5:

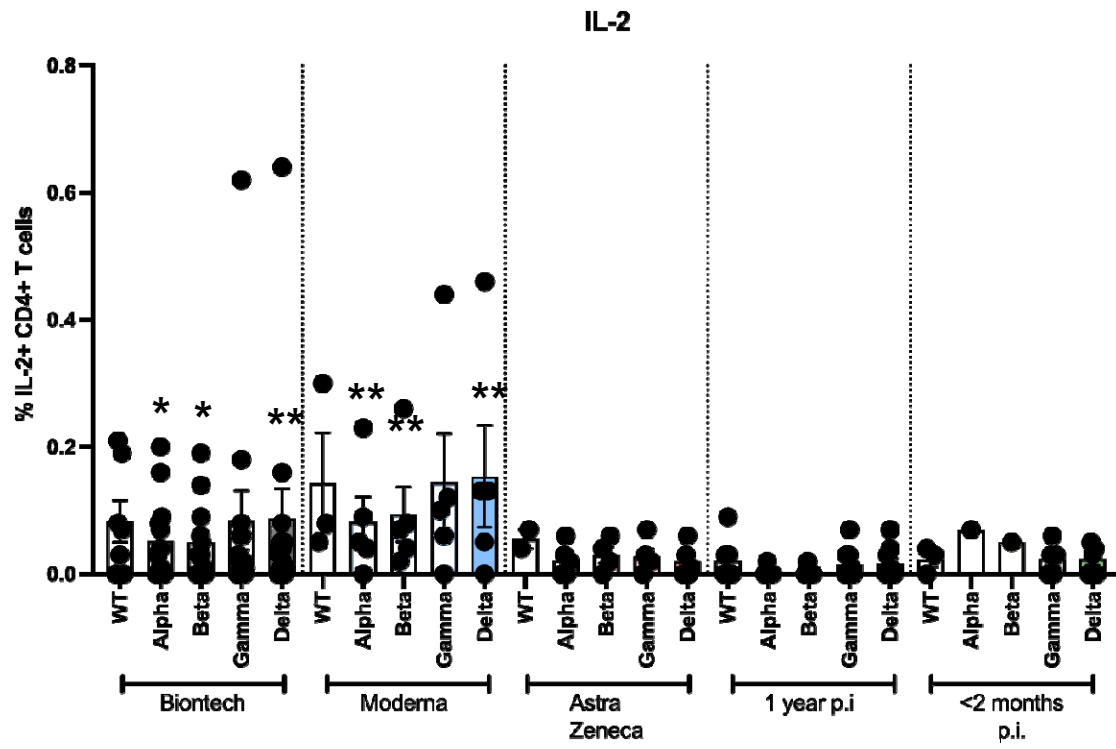


Figure 6:

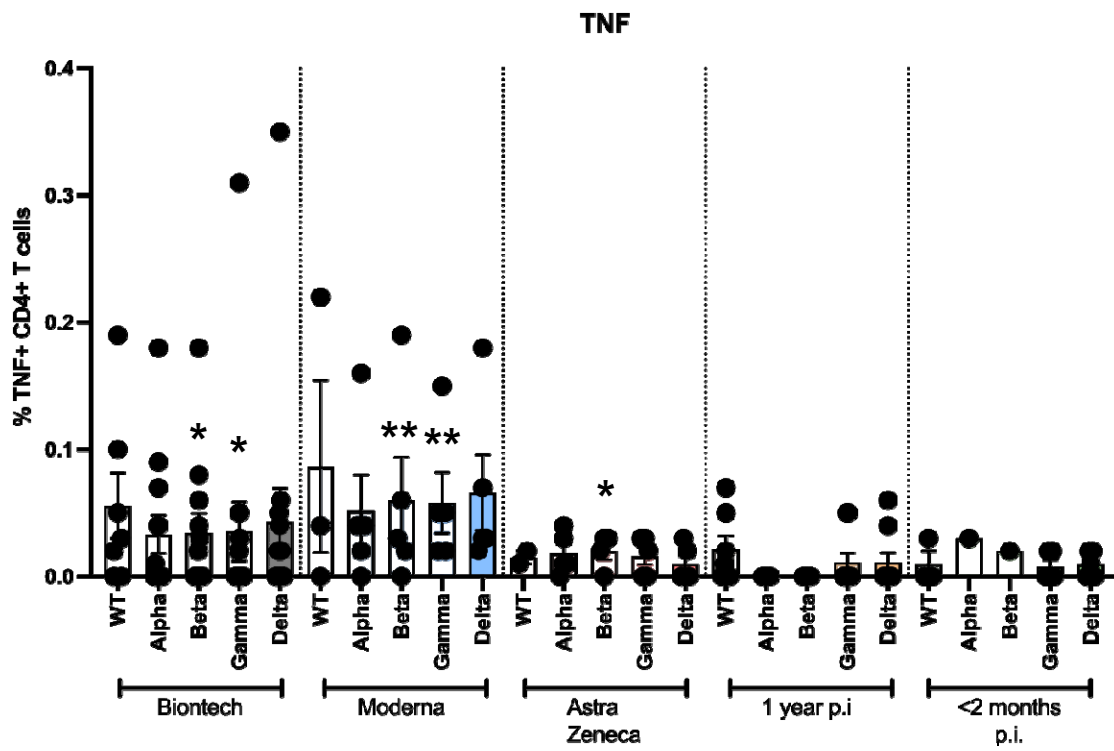


Table 1:

	Marker	Fluorochrome	Clone	Manufacturer	Cat. No.
Extracellular Staining	Live/dead	fixable Aqua	-	ThermoFisher	L34965
	CD3	VioBlue	BW264/56	Miltenyi	170-081-046
	CD4	APC	VIT4	Miltenyi	130-113-210
	CD8	PerCP	BW135/80	Miltenyi	130-113-160
Intracellular Staining	IFN	PE	45-15	Miltenyi	130-113-493
	CD154	FITC	5C8	Miltenyi	130-113-606
	TNF	PE-Vio770	cA2	Miltenyi	130-120-492
	IL-2	APC-Vio 770	REA689	Miltenyi	130-111-492